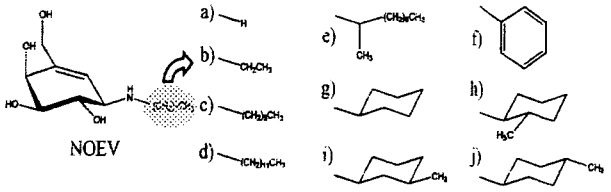

図1 シミュレーション実験に用いた化合物

C．研究結果と考察

ヒトβ-ガラクトシダーゼ構造の予測結果を図2に示す．ホモロジーモデリングの際に得られたヒトβ-ガラクトシダーゼとアオカビβ-ガラクトシダーゼのアラインメントでは，前半部分がより高い相同性を示し，両酵素の活性残基も一致していた．この前半部分が糖質分解酵素に良く見られるTIMバレルを構成しており，精度よく構造予測できたと考えられる．

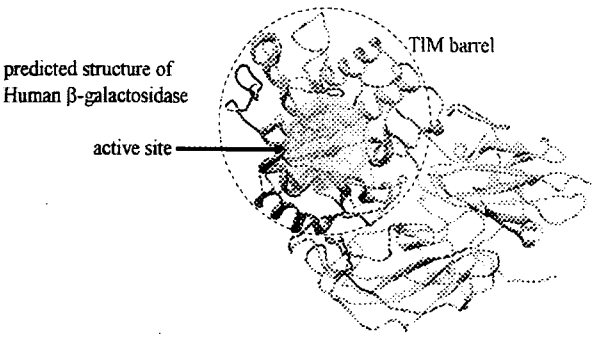

図2 ヒトβ-ガラクトシダーゼの予測構造

この構造にNOEVをドッキングさせた結果を図3に示す．また，各化合物の結合自由エネルギー予測結果を図4に示す．これら11種の化合物の中ではNOEVの結合自由エネルギーが最も低くなった．これはNOEVの結合強度が最も強いということであり，NOEVの最適性を示すことができた．また，残念ながらより結合強度の強い化合物の発見には至らなかった．

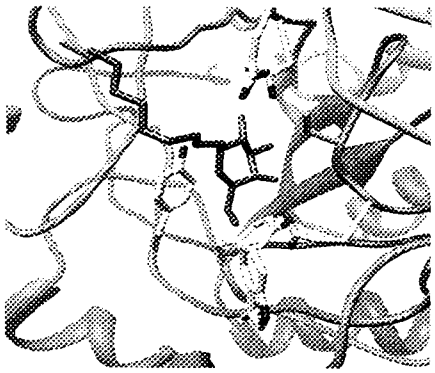

図3 ヒトβ-ガラクトシダーゼとNOEVのドッキング結果（紫：NOEV）

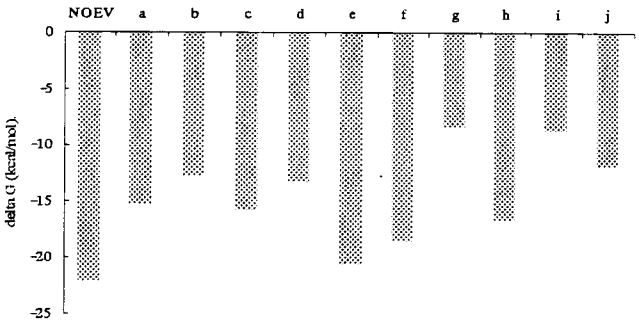

図4 各化合物の結合自由エネルギー予測結果

PROPKAを用いてイオン性残基のpKaを予測した結果を表1に示す．pH7からpH5の変化において水素化状態に変化のある残基，つまり，pKa>5である残基は131番目及び188番目のグルタミン酸のみであった．188番目のグルタミン酸残基は活性残基の一つで水素供与体である．つまり，ヒトβ-ガラクトシダーゼが正常に機能するためにはこの残基が水素を保持していなければならない．よってヒトβ-ガラクトシダーゼが正常に働くpH5の条件で188番目のグルタミン酸が水素化されるという予測は生物学的に妥当な結果であり，このPROPKAの結果をもとに水素付加されたヒトβ-ガラクトシダーゼがpH5の条件を再現しているという判断も信頼できると考えられる．

表1 PROPKAによるpKaの予測結果

(+: protonated, -: unprotonated)

	Predicted pKa	pH7	pH5
131GLU	6.32	-	+
188GLU (proton donor)	5.60	-	+
others	<5	-	-

上記の結果を受けて，131番目および188番目のグルタミン酸を水素付加状態にした酵素と188番目のグルタミン酸のみ水素付加状態にした酵素の2種の酵素を用意した．これらの酵素にNOEVをドッキングし，シミュレーションを実行したのち結合自由エネルギーを予測した．結果を表2に示す．この結果より，pH5ではpH7のときより結合自由エネルギーが高い，つまりライソゾーム内ではヒトβ-ガラクトシダーゼに対するNOEVの結合強度が弱くなると言うことができる．これはケミカルシャペロン療法において予想されている作用機序を支持する結果である．

表2　pH5における結合自由エネルギー予測結果

Protenated GLU	188	131 &188	None
pH	5	5	7
ΔG(kcal/mol)	-16.96	-16.57	-22.06

D．結論

NOEVおよび10種のNOEV類似化合物について，ヒトβ-ガラクトシダーゼに対する結合強度はNOEVが最も強いことを予測した．

pH7とpH5においてNOEVの結合強度に差があることを示し，ケミカルシャペロン療法の作用機序に対する示唆を得た．

E．研究発表

学会発表

1．徐広幸，柚木克之，榊原康文：Molecular simulations toward predicting free energy change of Human Beta-Galctosidase-NOEV complex，生物物理学会第45回年会，ポスター番号 1P044, 2007.

F．知的財産権の出願・登録状況

なし

別添5

研究成果の刊行に関する一覧表

書籍

著者氏名	論文タイトル名	書籍全体の編集者名	書　籍　名	出版社名	出版地	出版年	ページ
Suzuki Y, Nanba E, Matsuda J, Oshima A	β-Galactosidase deficiency (β-galactosidosis): G_{M1}-Gangliosidosis and Morquio B disease.	Valle D, Beaudet AL, Vogelstein B, Kinzler KW, Antonarakis SF, Ballabio A	The Online Metabolic and Molecular Bases of Inherited Disease	McGraw-Hill	New York	2008	<http://www.ommbid.com/>

雑誌

発表者氏名	論文タイトル名	発表誌名	巻号	ページ	出版年
Takamura A, Higaki K, Kajimaki K, Otsuka S, Ninomiya H, Matsuda J, Ohno K, Suzuki Y, Nanba E	Enhanced autophagy and mitochondrial aberrations in murine G_{M1}-gangliosidosis.	Biochem Biophys Res Commun	367	616-622	2008
Shimotori M, Maruyama H, Nakamura G, Suyama T, Sakamoto F, Itoh M, Miyabayashi S, Ohnishi T, Sakai N, Wataya-Kaneda M, Kubota M, Takahashi T, Mori T, Tamura K, Kageyama S, Shio N, Maeba T, Yahagi H, Tanaka M, Oka M, Sugiyama H, Sugawara T, Mori N, Tsukamoto H, Tamagaki K, Tanda S, Suzuki Y, Shinonaga C, Miyazaki J, Ishii S, Gejyo F	Novel mutations of the GLA gene in Japanese patients with Fabry disease and their functional characterization by active site specific chaperone.	Hum Mutat	29	331	2008
Suzuki Y	Chemical chaperone therapy for G_{M1}-gangliosidosis.	Cell Molec Life Sci	10	351-353	2008
Ishii S, Chang H-H, Kawasaki K, Yasuda K, Wu H-L, Garman SC, Fan J-Q	Mutant α-galactosidase A enzymes identified in Fabry disease patients with residual enzyme activity: biochemical characterization and restoration of normal intracellular processing by 1-deoxygalactonojirimycin.	Biochem J	406	285-295	2007

Fan J-Q, Ishii S	Active-site-specific chaperone therapy for Fabry disease: Yin and Yang of enzyme inhibitors.	FEBS J	274	4962-4971	2007
Suzuki Y, Ichinomiya S, Kurosawa M, Ohkubo M, Watanabe H, Iwasaki H, Matsuda J, Noguchi Y, Takimoto K, Itoh M, Tabe M, Iida M, Kubo T, Ogawa S, Nanba E, Higaki K, Ohno K, Brady RO	Chemical chaperone therapy: clinical effect in murine G_{M1}-gangliosidosis.	Ann Neurol	62	671-675	2007
Ogawa S, Kanto M, Suzuki Y	Development and medical application of unsaturated carbaglycosylamine glycosidase inhibitors.	Mini-Rev Med Chem	7	679-691	2007
Ichinomiya S, Watanabe H, Maruyama K, Toda H, Iwasaki H, Kurosawa M, Matsuda J, Suzuki Y	Motor and reflex testing in G_{M1}-Gangliosidosis model mice.	Brain Dev	29	210-216	2007
Lei K, Ninomiya H, Suzuki M, Inoue T, Sawa M, Iida M, Ida H, Eto Y, Ogawa S, Ohno K, Kaneski C, Brady RO, Suzuki Y	Enzyme enhancement activity of *N*-octyl-β-valienamine on β-glucosidase mutants associated with Gaucher disease.	Biochim Biophys Acta	1772	587-596	2007
Suzuki M, Sugimoto Y, Ohsaki Y, Ueno M, Kato S, Kitamura Y, Hosokawa H, Davies JP, Ioannou YA, Vanier MT, Ohno K, Ninomiya H	Endosomal accumulation of Toll-like receptor 4 causes constitutive secretion of cytokines and activation of signal transducers and activators of transcription in Niemann-Pick disease type C (NPC) fibroblasts: a potential basis for glial cell activation in the NPC brain.	J Neurosci	27	1879-1891	2007

研究成果による特許権等の知的財産権の出願・登録状況

なし

健康危険情報

なし

研究成果の刊行物・別刷

Scriver's OMMBID The Online Metabolic & Molecular Bases of Inherited Disease
Editors: Valle • Beaudet • Vogelstein • Kinzler • Antonarakis • Ballabio
Editors Emeritus: Scriver • Childs • Sly

PART 4: LYSOSOMAL DISORDERS

Chapter 151: β-Galactosidase Deficiency (β-Galactosidosis): G_{M1}

$_{M1}$ Yoshiyuki Suzuki, Eiji Nanba, Junichiro Matsuda, Akihiro Oshima

Abstract

1. Hereditary deficiency of lysosomal acid β-galactosidase (β-galactosidosis) is expressed clinically as two different diseases, G_{M1} gangliosidosis and Morquio B disease. The mode of inheritance is autosomal recessive. G_{M1} gangliosidosis is a neurosomatic disease occurring mainly in early infancy (infantile form; type 1). Developmental arrest is observed a few months after birth, followed by progressive neurologic deterioration and generalized rigospasticity with sensorimotor and psychointellectual dysfunctions. Macular cherry-red spots, facial dysmorphism, hepatosplenomegaly, and generalized skeletal dysplasia are usually present in infantile cases. Cases of later onset have been described as late infantile/juvenile form (type 2) or adult/chronic form (type 3). They are observed as progressive neurologic diseases in childhood or in young adults. Dysmorphic changes are less prominent or absent in these clinical forms, although vertebral dysplasia is often detected by radiographic studies. No specific neurologic manifestations are known for late infantile/juvenile patients with G_{M1} gangliosidosis. Extrapyramidal signs of protracted course, mainly presenting as dystonia, are the major neurologic manifestation in adults with G_{M1} gangliosidosis.

2. Morquio B disease is clinically a mild phenotype of Morquio A disease. It is expressed as generalized skeletal dysplasia with corneal clouding, resulting in short stature, pectus carinatum (sternal protrusion), platyspondylia, odontoid hypoplasia, kyphoscoliosis, and genu valgum. There is no central nervous system involvement, although spinal cord compression may occur at the late stage of the disease. Intelligence is normal, and hepatosplenomegaly is not present. X-ray changes are of pathognomonic significance.

3. There is diffuse atrophy of the brain in patients with early onset G_{M1} gangliosidosis. Neurons are filled with numerous membranous cytoplasmic bodies (MCB), and inclusions of other types are observed in glial cells: pleomorphic lipid bodies, membranovesicular bodies, or large compact oval deposits. There are histiocytes with distended cytoplasm in visceral organs. Cytoplasmic inclusions observed under electron microscopy are different from MCB in neurons. They are vacuoles filled with fine granular, tubular, or amorphous osmiophilic material. These changes are less prominent in cases of mild phenotypic expression.

4. Glycoconjugates with terminal β-galactose are increased in tissues and urine from patients with G_{M1} gangliosidosis and Morquio B disease. Ganglioside G_{M1} and its asialo derivative G_{A1} accumulate in the G_{M1} gangliosidosis brain. High amounts of oligosaccharides derived from keratan sulfate or glycoproteins have been reported in visceral organs and urine from G_{M1} gangliosidosis or Morquio B disease patients. Undersulfated keratan sulfate has also been described.

5. Two lysosomal enzymes are known for hydrolysis of terminal β-linked galactose at acidic pH in various glycoconjugates. One is an enzyme usually called β-galactosidase (EC 3.2.1.23), catabolizing ganglioside G_{M1}, galactose-containing oligosaccharides, keratan sulfate, and other β-galactose-containing glycoconjugates (G_{M1} β-galactosidase). The enzyme activity is markedly reduced or almost completely deficient in cells and body fluids from patients with β-galactosidosis. Heterogeneous kinetic or physicochemical properties have been found in the mutant enzymes. The

degree of substrate storage and residual enzyme activity is correlated with the severity of each clinical phenotype; infantile G_{M1} gangliosidosis shows the highest substrate storage and the lowest residual enzyme activity as compared with other milder phenotypes. The second genetically different β-galactosidase is galactosylceramidase (galactocerebrosidase; EC 3.2.1.46), catabolizing galactosylceramide, galactosylsphingosine, and other lipid compounds. Genetic deficiency of this enzyme results in globoid cell leukodystrophy, which is another neurometabolic disease.

6. The human β-galactosidase gene has been mapped on chromosome 3 (3p21.33). The cDNA codes for a protein of 677 amino acids, including a putative signal sequence of 23 amino acids and 7 potential asparagine-linked glycosylation sites. The gene spans more than 60 kb, and contains 16 exons. The promoter has the characteristics of a housekeeping gene, with GC-rich stretches and 5 SP1 transcription elements on the two strands. Molecular genetic analysis revealed heterogeneous gene mutations in all clinical forms of β-galactosidosis, such as missense/nonsense mutation, insertion/duplication, and insertion causing splicing defect. Neither the type nor location of mutation in the gene is correlated to the clinical phenotype. Five common mutations have been known: R482H in Italian patients with infantile G_{M1} gangliosidosis; R208C in American patients with infantile G_{M1} gangliosidosis, R201C in Japanese patients with juvenile G_{M1} gangliosidosis; I51T in Japanese patients with adult G_{M1} gangliosidosis; and W273L in Caucasian patients with Morquio B disease. Restriction analysis has been successfully performed for the diagnosis of the common mutations in new patients.

7. Morphologic, pharmacologic, and biochemical aberrations have been found in the brain of G_{M1} gangliosidosis patients and animals. Meganeurites and ectopic dendrogenesis are observed in G_{M1} gangliosidosis, and the extent of meganeurite development is related to the onset, severity, and clinical course of the disease. Various pharmacologic abnormalities have been observed in feline G_{M1} gangliosidosis, such as cholinergic dysfunction, neuroaxonal dystrophy in GABAergic neurons, and alteration of phospholipase C and adenyl cyclase activities. These data suggest that morphologic and metabolic effects occur in the presence of excessive storage of ganglioside G_{M1}

8. G_{M1} gangliosidosis has been recorded in cats, dogs, sheep, and calves. These animals showed various central nervous system manifestations. β-Galactosidase is deficient, and storage of G_{M1} and oligosaccharides has been confirmed. Furthermore, mouse models have been generated by disruption of the β-galactosidase gene. The β-galactosidase-deficient knockout mouse presented with progressive neurologic manifestations a few months after birth. Clinical, pathologic, and biochemical analysis indicated that this also is an authentic model of human G_{M1} gangliosidosis. In addition, phenotype-specific model mice have been produced by introducing human mutant genes, resulting in various clinical forms of β-galactosidosis (knockout-transgenic mice). These mice models are used for new therapeutic approaches to human β-galactosidosis patients.

9. The mouse model of juvenile G_{M1}-gangliosidosis expressing the R201C mutation was used for a new molecular therapy using a low-molecular-weight compound, N-octyle-4-epi-β-valienamine (NOEV). Orally fed NOEV passed through the blood-brain barrier, enhanced the deficient β-galactosidase activity, and induced degradation of G_{M1} and G_{A1} in the central nervous system. This new molecular therapy (chemical chaperone therapy) will be useful for certain patients with β-galactosidosis and potentially other lysosomal storage diseases with central nervous system involvement.

HISTORY

In 1959, Norman et al.[1] reported a patient with a specific form of amaurotic idiocy—"Tay-Sachs disease with visceral involvement." Clinical and pathologic findings resembled those of Tay-Sachs disease, but

Available online at www.sciencedirect.com
ScienceDirect
Biochemical and Biophysical Research Communications 367 (2008) 616–622
BBRC
www.elsevier.com/locate/ybbrc

Enhanced autophagy and mitochondrial aberrations in murine G_{M1}-gangliosidosis

Ayumi Takamura [a,b], Katsumi Higaki [a,*], Kenya Kajimaki [a,c], Susumu Otsuka [a,d], Haruaki Ninomiya [e], Junichiro Matsuda [f], Kousaku Ohno [g], Yoshiyuki Suzuki [h], Eiji Nanba [a]

[a] Division of Functional Genomics, Research Center for Bioscience and Technology, Tottori University, 86 Nishi-machi, Yonago 683-8503, Japan
[b] Department of Biosignaling, School of Life Sciences, Tottori University, 86 Nishi-machi, Yonago 683-8503, Japan
[c] Department of Molecular and Cellular Biology, School of Life Sciences, Tottori University, 86 Nishi-machi, Yonago 683-8503, Japan
[d] Department of Biomedical Science, Institute of Regenerative Medicine and Biofunction, Graduate School of Medical Science, Tottori University, 86 Nishi-machi, Yonago 683-8503, Japan
[e] Department of Biological Regulation, School of Health Science, Faculty of Medicine, Tottori University, 86 Nishi-machi, Yonago 683-8503, Japan
[f] National Institute of Biomedical Innovation, 7-6-8 Saito-asagi, Ibaraki, 567-0085, Japan
[g] Division of Child Neurology, Tottori University Faculty of Medicine, 36-1 Nishi-machi, Yonago 683-8504, Japan
[h] Graduate School, International University of Health and Welfare, 2600-1 Kita-Kanemaru, Otawara 324-8501, Japan

Received 28 December 2007
Available online 9 January 2008

Abstract

G_{M1}-gangliosidosis is an autosomal recessive lysosomal lipid storage disorder, caused by mutations of the lysosomal β-galactosidase (β-gal) and results in the accumulation of G_{M1}. The underlying mechanisms of neurodegeneration are poorly understood. Here we demonstrate increased autophagy in β-gal-deficient (β-gal$^{-/-}$) mouse brains as evidenced by elevation of LC3-II and beclin-1 levels. Activation of autophagy in the β-gal$^{-/-}$ brain was found to be accompanied with enhanced Akt–mTOR and Erk signaling. In addition, the mitochondrial cytochrome *c* oxidase activity was significantly decreased in brains and cultured astrocytes from β-gal$^{-/-}$ mouse. Mitochondria isolated from β-gal$^{-/-}$ astrocytes were morphologically abnormal and had a decreased membrane potential. These cells were more sensitive to oxidative stress than wild type cells and this sensitivity was suppressed by ATP, an autophagy inhibitor 3-methyladenine and a pan-caspase inhibitor z-VAD-fmk. These results suggest activation of autophagy leading to mitochondrial dysfunction in the brain of G_{M1}-gangliosidosis.

Keywords: G_{M1}-gangliosidosis; Lysosome; Autophagy; mTOR; Mitochondria; Astrocyte; Neurodegeneration

G_{M1}-gangliosidosis (OMIM 230500) is an autosomal recessive lysosomal lipid storage disorder with progressive central nervous system dysfunction, visceromegaly, and skeletal dysplasias. It is caused by deficiency of lysosomal acid β-galactosidase (β-gal) due to mutations in the *GLB1* gene [1]. Three clinical forms (infantile, juvenile, and adult/chronic) have been distinguished according to the age of onset and severity, mainly due to different residual activities of the mutant enzymes and hence different levels of the substrate accumulation in tissues, especially in the brain. Pathologically, typical lamellar inclusions or membranous cytoplasmic bodies are found in neurons of human, mouse, and other animal models of G_{M1}-gangliosidosis [2–4]. Neurons are the primary target of storage, but astrocytes may also appear abnormally vacuolated [5]. Recently, we have developed chemical chaperone therapy for brain pathology in G_{M1}-gangliosidosis [6,7]. However,

Abbreviations: LC3, microtubule-associated protein 1 light chain 3; mTOR, mammalian target of rapamycin; PI3K, phosphatidylinositol 3 kinase; LDH, lactate dehydrogenase; 3-MA, 3-methyladenine; DMEM, Dulbecco's modified Eagle's medium; PBS, phosphate-buffered saline; BSA, bovine serum albumin.

* Corresponding author. Fax: +81 859 38 6470.
E-mail address: kh4060@grape.med.tottori-u.ac.jp (K. Higaki).

0006-291X/$ - see front matter © 2008 Elsevier Inc. All rights reserved.
doi:10.1016/j.bbrc.2007.12.187

underlying biological mechanisms responsible for neurodegeneration still remain uncertain [8].

Macroautophagy (hereafter referred to as autophagy) involves bulk degradation of complete regions of the cytosol [9]. The target regions are initially sequestered in multimembrane vacuoles, known as autophagosome which eventually fused with lysosomes for degradation. Autophagy plays a cytoprotective role in low-nutrient conditions and disease states by catabolizing intracellular substrates for energy supply and by removing failing mitochondria and other factors that trigger cell death [10]. Dysfunction of autophagy can disrupt neuronal function and ultimately lead to neurodegeneration [11].

In this study, we demonstrate enhanced autophagy and mitochondrial alterations in the G_{M1}-gangliosidosis mouse brain, which might lead to neurodegeneration in this disease.

Materials and methods

Antibodies and reagents. Monoclonal anti-G_{M1} (GMB16) was from Seikagaku Corp. (Tokyo, Japan), polyclonal anti-LC3 (PD014) was from MBL International Corp. (Woborn, MA, USA), polyclonal anti-beclin-1 (H-300) was from Santa Cruz Biotechnology Inc. (Santa Cruz, CA, USA) and polyclonal anti-Atk, anti-phospho-Akt (Ser473), anti-mTOR, anti-phospho-mTOR (Ser2448), anti-S6 ribosomal protein (5G10), and anti-phospho-S6 ribosomal protein (Ser235/236) were from Cell Signaling Technology (Boston, MA, USA). Paraquat, ATP and chloroquine were purchased from Wako (Tokyo, Japan), 3-methyladenine (3-MA), and rapamycin were from Sigma (St. Louis, MO, USA) and z-VAD-fmk was from Promega (Madison, WI, USA).

Mice and tissue collection. A C57BL/6-based congenic mouse strain with β-gal-deficiency (β-gal$^{-/-}$) was established as reported previously [3,6]. All animal procedures were carried out following the protocols approved by the committee for animal experiments in Tottori University and β-gal$^{-/-}$ mice was obtained by cross bleeding. For tissue staining, mice were anesthesized and perfused with 4% paraformaldehyde (PFA) in sodium phosphate, pH 7.4. Brains were embedded in OTC compound (Sakura Finetechnical Co., Tokyo, Japan) and 8 μm sections were cut using a cryostat. For protein extractions, tissues were removed and frozen in liquid nitrogen.

Primary culture of astrocytes. For astrocyte preparation, brains from postnatal day four mice were removed under anesthesia. The cerebral cortex was dissociated and cells were seeded on plastic dishes in DMEM-F12 supplemented with 15% fetal bovine serum (FBS). They were cultured for 7 days, trypsinized, and seeded on dishes with DMEM-F12 with 10% FBS. They were confirmed to be GFAP-positive astrocytes at 3 weeks by immunostaining with polyclonal anti-GFAP (data not shown). Lactate dehydrogenase (LDH) cytotoxicity assay (Wako, Tokyo, Japan) was performed following the manufacturer's instruction.

Immunoblot analysis. Mouse brains were lysed by sonication in a buffer containing 10 mM Tris–HCl (pH 7.4), 150 mM NaCl, 1 mM EDTA, 1 mM EGTA plus protease inhibitor cocktail (Roche). Protein was quantified using Color-Producing Solution (Wako). Samples were separated on 10% SDS–PAGE and transferred on a nylon membrane (Millipore) using a semi-dry transfer blotter (BioRad). Membranes were incubated in a polyclonal antibody followed by a horseradish peroxidase-linked donkey anti-rabbit IgG antibody (Amersham). Detection was performed using ECL (Amersham Pharmacia Biotech) and images were captured in X-ray film or a LAS-1000 plus imager (Fujifilm).

Immunofluorescence staining. Brain sections were permiabilized with 0.25% Triton X-100 in PBS for 15 min at room temperature, blocked with 1% BSA in PBS for 1 h at room temperature, and incubated with the first antibody at 4 °C overnight. Bind antibodies were detected with Alexafluor-conjugated secondary antibody for 1 h at room temperature. Fluorescence images were obtained using confocal microscopy (Leica, TCS-SP2; Wetzler, Germany).

Mitochondrial assay. Mitochondria were isolated from the mouse brain and cultured astrocytes using mitochondrial isolation kit (BioChain Ins. Hayward, CA, USA) and the enzyme activity of cytochrome *c* oxidase was determined using mitochondrial activity kit (BioChain Ins.) following the manufacturer's instruction. For mitochondrial labeling, cultured astrocytes were seeded on sterile cover slips or glass base dishes (Iwaki, Tokyo, Japan) and incubated in Hanks' balanced salt solution containing 100 nM MitoTracker Red CMXRos or 3 μM Mitotracker JC-1 (MolecularProbes Inc., Eugene, OR, USA) for 20 min at 37 °C. Cells were then washed with Hanks' balanced salt solution and fluorescent images were obtained using confocal microscopy.

Results

G_{M1} accumulation and sequestration of autophagosomes proteins in the β-gal$^{-/-}$ mice brain

Microtubule-associated protein 1 light chain 3 (LC3), a mammalian homolog of the yeast autophagic protein Atg8, has been used as an autophagosomal marker [9]. Cleavage of LC3 in its carboxy terminal gives rise to a cytosolic soluble form LC3-I which is further modified into LC3-II, a protein that associate with autophagosomes. Brain levels of LC3 were assessed by immunoblotting. Although levels of LC3-I and LC3-II in β-gal$^{-/-}$ mice did not significantly differ from those in wild type (WT) mice at 10-day-old, the level of LC3-II were significantly higher in mutant mice at 10 months of age (Fig. 1A). G_{M1} and LC3 double immunofluorescence showed co-localization of LC3-immunopositive-granules with G_{M1} in neurons of β-gal$^{-/-}$ mice at 10 months (Fig. 1B). Beclin-1 is the mammalian ortholog of yeast Atg6, and is a part of the Class III phosphatidylinositol 3 kinase (PI3K) complex that participate in autophagosome formation [9]. The level of beclin-1 was increased in brain lysates from 10-month-old β-gal$^{-/-}$ mice when compared to WT mice (Fig. 1C and D). The Akt/mammalian target of rapamycin (mTOR) and the extracellular signal kinase (Erk) are two major pathways that regulate autophagy [10,12]. Phsphorylation of Akt, Erk, and mTOR were increased, whereas no obvious alteration of S6 was detected in the brain lysates of β-gal$^{-/-}$ mice at 10 months (Fig. 2A and B).

Mitochondrial alterations in β-gal$^{-/-}$ mice

Autophagy is a highly regulated process that is involved in the turnover of long-lived proteins and whole organelles. It can specifically target distinct organelles, such as mitochondria in mitopathy and the endoplasmic reticulam in reticulopathy [9]. We next sought to examine whether sequestration in autophagic vacuoles affects mitochondrial function in this mouse model. The level of mitochondrial cytochrome *c* oxidase activity was significantly decreased in the brain of β-gal$^{-/-}$ mice than that of WT mice at 10 months (Fig. 3A). Similarly, cultured astrocytes from

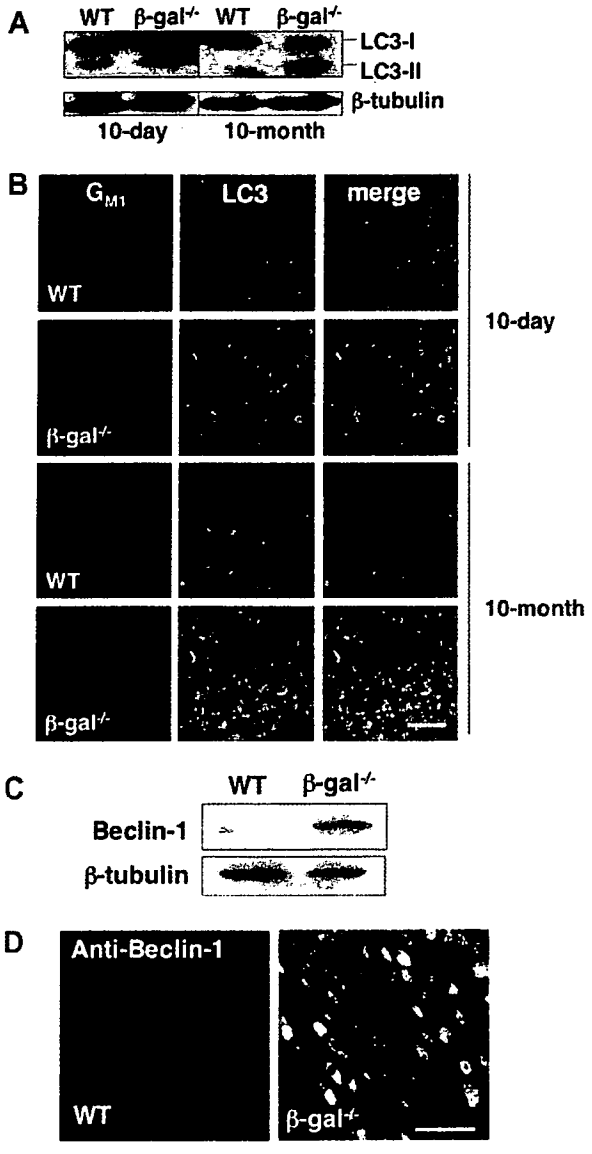

Fig. 1. Elevation of LC3-II and beclin-1 expression in β-gal$^{-/-}$ mouse brain. Cerebellar lysates from WT and β-gal$^{-/-}$ mice were subjected to Western blotting with anti-LC3 (A) or anti-beclin-1 (C). Immunofluorescence of cellular distribution of LC3 (B) and beclin-1 (D) proteins in the frontal cerebral cortex of WT and β-gal$^{-/-}$ mice. Scale bar = 80 μm.

β-gal$^{-/-}$ mice showed lysosomal accumulation of G_{M1} and elevated LC3-II and beclin-1 levels (data not shown), and it had a decreased cytochrome *c* oxidase activity (Fig. 3A). Next, the morphology and the membrane potential of mitochondria were examined in cultured astrocytes using confocal microscopy. There were obvious differences in mitochondrial morphology between WT and β-gal$^{-/-}$ astrocytes. In WT astrocytes, mitochondria were organized as extended tubular structures, whereas β-gal$^{-/-}$ astrocytes contained smaller, fragmented or circulated mitochondria (Fig. 3B and C). When cells were stained with Mitotracker JC-1, a marker of the mitochondrial membrane potential,

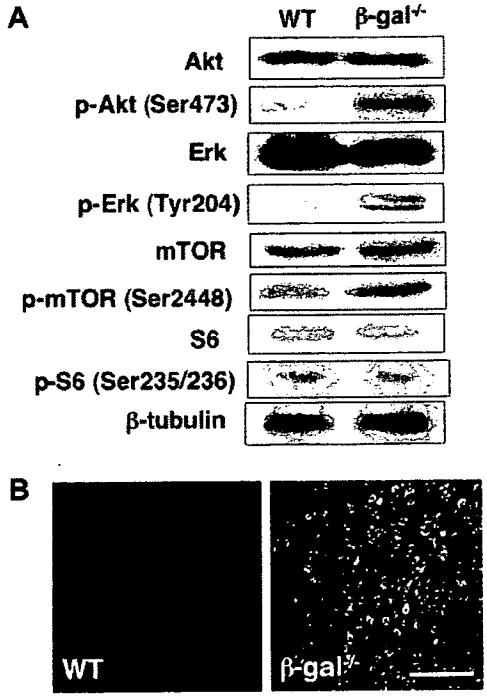

Fig. 2. Changes in Akt/mTOR and Erk signals in β-gal$^{-/-}$ mouse brain. (A) Cerebellar lysates from postnatal of 10-month-old WT and β-gal$^{-/-}$ mice were subjected to Western blotting with indicated antibodies. (B) Cellular distribution of p-mTOR (Ser2448) in the frontal cerebral cortex of WT and β-gal$^{-/-}$ mice at 10 months of age. Scale bar = 80 μm.

the intensity of red and green fluorescence was decreased in β-gal$^{-/-}$ astrocytes compared to the WT (Fig. 3D).

Dysfunction of autophagic-lysosomal pathways and mitochondria

To examine functional relevance of mitochondrial dysfunction to cell death, we treated cultured astrocytes with oxidative stress reagent paraquat. LDH release assay revealed a significant increase of the percentage of dead cells was noted in β-gal$^{-/-}$ astrocytes compared to that in WT cells (Fig. 4A). We also attempted to characterize the impairment in autophagy and mitochondria in β-gal$^{-/-}$ astrocytes. LDH release in paraquat (250 μM)-treated-β-gal$^{-/-}$ astrocytes was significantly suppressed by addition of 0.5 mM ATP in the medium for 24 h (Fig. 4B). We next examined effects of 3-MA and rapamycin, which inhibit or induce autophagy, respectively [13], 3-MA at 10 mM reduced paraquat-induced-LDH release in β-gal$^{-/-}$ astrocytes, whereas, rapamycin (2 μg/ml) had no effects on cell death. We also examined a cell-permeable pan-caspase inhibitor, z-VAD-fmk, since autophagic cell death was partly mediated by caspase activation [10]. z-VAD-fmk (100 μM) significantly decreased cell death in paraquat-treated-β-gal$^{-/-}$ astrocytes. Under these conditions, none of the drugs affected LDH release in

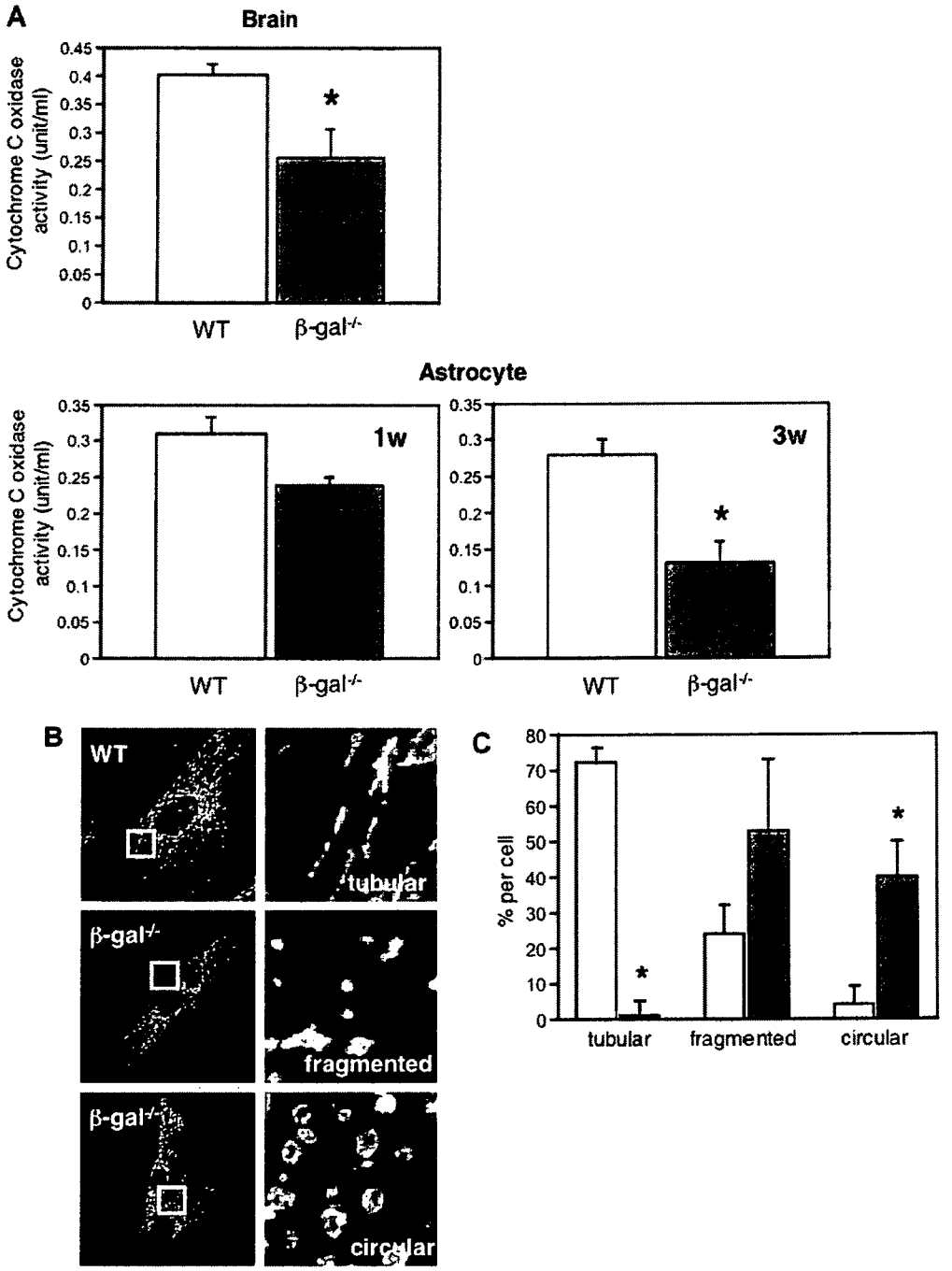

Fig. 3. Mitochondrial alteration in β-gal$^{-/-}$ mouse brain and astrocyte. (A) Levels of cytochrome *c* oxidase activities in extracts from the brain and primary astrocytes of WT and β-gal$^{-/-}$ mice. Values are means ± SEM from three independent experiments, $^{*}p < 0.01$ significantly differ from the value of WT cells. (B) Primary astrocytes from neonatal WT and β-gal$^{-/-}$ cortex were cultured for 3 weeks and labeled with MitoTracker Red. Morphological analysis of mitochondria was obtained using confocal microscopy. (C) The number of cells with each morphology of mitochondria was computed. Values for the percent of total cell number from three independent experiments. $n = 30$ cells and values are means ± SEM. (open bars: WT; dark bars: β-gal$^{-/-}$) (D) Primary-cultured astrocytes were labeled with JC-1. Shown are the representative images obtained by confocal microscopy using red and green channels. Scale bar = 25 μm. (For interpretation of the references to color in this figure legend, the reader is referred to the web version of this paper.)

WT astrocytes. Chloroquine, an inhibitor of autophagosome–lysosome fusion, induced cell death in WT astrocytes after treatment with paraquat, and this cell death was suppressed by ATP, 3-MA and z-VAD-fmk (Fig. 4B).

Discussion

One of the most important functions of autophagy is to maintain cellular energy subjected to nutrient deprivation

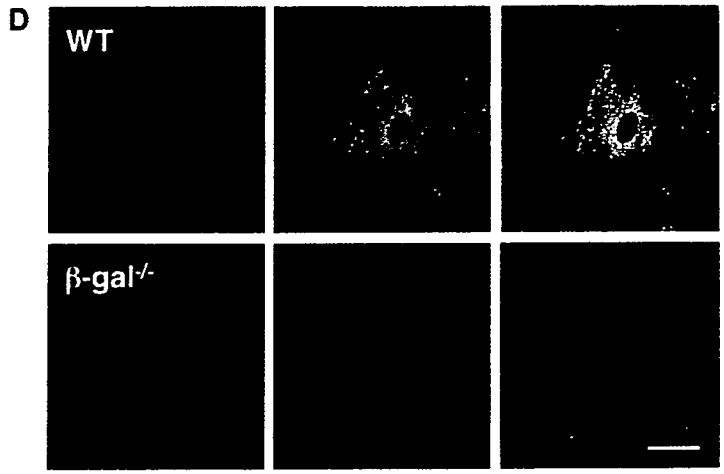

Fig. 3 (*continued*)

and potentially other forms of stress. Autophagy is a highly regulated process that is involved in the turnover of long-lived proteins and cytoplasmic constituents including mitochondria, endoplasmic reticulum, and ribosomes [10]. Molecular mechanisms that regulated autophagy in yeast and mammalian have recently been identified [9]. Knockout of autophagy genes causes abnormal accumulation in ubiquitinated inclusions and neurodegeneration in mice and that implicates in mechanisms of neurodegeneration [14,15].

In the present study, we showed increased levels of autophagic proteins in the β-gal$^{-/-}$ mice brain. Immunoblot analysis revealed an increase in levels of LC3-II, a widely used marker for autophagy, in all brain areas examined at 10 months of age. Levels were particularly high in cerebellum and brain stem, where severe neuronal death occurs in the β-gal-deficient human and mouse brain [1,3,4]. Increased autophagic stress was further confirmed by the presence of LC3-positive structures in cells with intracellular G_{M1} accumulations. This induction of autophagy was associated with increased expression of beclin-1. Beclin-1 is the mammalian ortholog of yeast Atg6, and is a part of the Class III PI3K machinery that participates in autophagosome formation [9].

Enhanced autophagy was recently reported in human skin fibroblasts and mice models of other types of lysosomal storage diseases, such as Danon disease [16], neuronal ceroid lipofuscinosis 2 [17], Pompe disease [18], mucolipidosis type IV [19] multiple sulfatase deficiency, mucopolysaccharidosis type IIA [20]. Induction of autophagy was also observed in the Niemann-Pick C1 (NPC1) mouse brain, which contained increased levels of beclin-1 [21].

The Akt–mTOR and Erk signaling pathways were also activated in β-gal$^{-/-}$ mice. Insulin signaling stimulates phosphorylation and activity of mTOR via Akt/PBK pathway and thereby represses autophagy in response to insulin-like and other growth factor signals [9]. Activation of these pathways is known to induce autophagy, although detailed mechanisms are still unknown. [12]. Previous studies have demonstrated localization of the active form of Erk in autophagosomes and mitochondria in degenerating brain [22], and that might happen in β-gal$^{-/-}$ brain.

Decrease in the cytochrome *c* oxidase activity, the morphological abnormality and high sensitivity to oxidative stress in the β-gal$^{-/-}$ astrocytes suggest mitochondrial abbreviations in this mouse. Inefficient autophagic-lysosomal fusion may cause accumulation of fragmented mitochondria. It is also possible that enhanced autophagy disrupted mitochondrial function. We showed that oxidative stress-induced cell death was suppressed by ATP, an autophagy inhibitor and a pan-caspase inhibitor in β-gal$^{-/-}$ astrocytes as well as in chloroquine-treated WT astrocytes, supporting the idea that enhanced autophagy induces mitochondrial dysfunction that leads to cell death. Mechanisms leading to cell death in astrocytes remain unclear, since functional relationship between autophagic cell death (also known as type II cell death) and apoptotic cell death (or type I cell death) is complex [10]. Autophagy and apoptosis may be triggered by common signals.

Autophagy has emerged as the major pathway involved in a number of neurodegenerative diseases, including Alzheimer disease [23], Parkinson disease [24], Huntington disease [25], and lysosomal storage diseases [16–21]. In each case, autophagic vacuoles accumulate in the affected neurons, indicating that activation of autophagy is a common feature of these diseases. However, the precise mechanisms leading to activation of autophagy remain elusive. Further investigation is warranted to clarify the mechanisms of enhanced autophagy in these disorders.

In summary, we provided evidence for abnormal activation of autophagy accompanied with mitochondrial alterations in the murine model of G_{M1}-gangliosidosis. Modulation of activity of autophagy and restoring mitochondrial functions may be of therapeutic benefit for this disease.

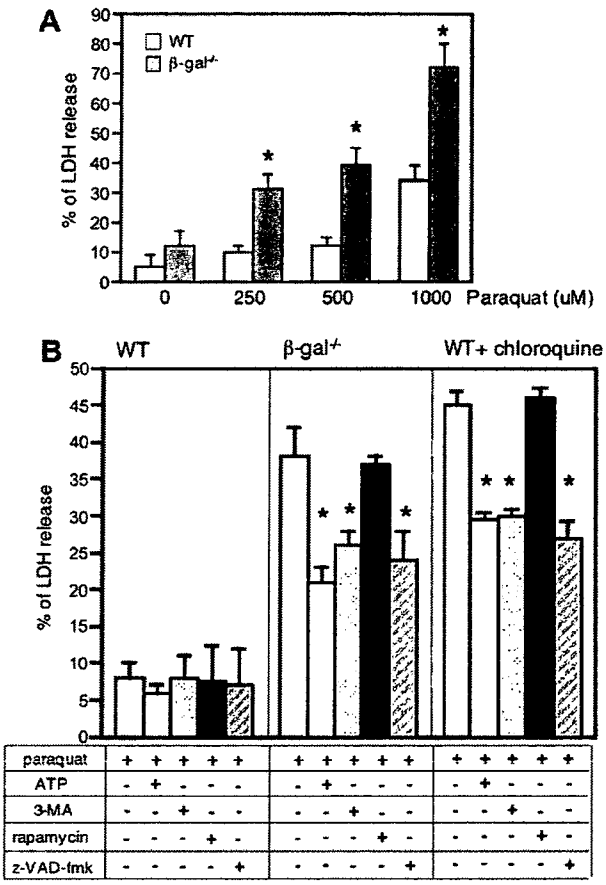

Fig. 4. Effects of ATP, 3-MA, rapamycin and a pan-caspase inhibitor on oxidative stress-induced cell death of astrocyte. (A) Lactate dehydrogenase (LDH) release assay. Astrocytes were cultured with or without paraquat for 24 h and the medium was collected for LDH release assay. Values were expressed as relative to the values from cells treated with 1% Tween 20. Each bar represents the mean (SEM) from three independent experiments. $^{*}p < 0.01$ significantly differ from the value of WT cells. (B) Both WT, β-gal$^{-/-}$ and chloroquine-treated WT astrocytes were treated with indicated drugs. LDH release assay were performed after 24 h treatment. Each bar represents the mean (SEM) from three independent experiments. $^{*}p < 0.01$ significantly differ from the value of paraquat-treated cells.

Acknowledgments

This work was supported by grants from Ministry of Education, Culture, Science, Sports, and Technology of Japan (13680918, 14207106, 16300141, 18390279, and 18790719) and Ministry of Health, Labour and Welfare of Japan (H10-No-006, H14-Kokoro-017, and H17-Kokoro-019).

References

[1] A. Oshima, E. Nanba, J. Matsuda, Y. Suzuki, β-Galactosidase deficiency (β-galactosidosis): GM1-gangliosidosis and Morquio B disease. In: D. Valle, A.L. Baudet, B. Vogelstein, et al., (Eds.), The Online Metabolic and Molecular Bases of Inherited Disease. 8th ed. McGraw-Hill, New York, 2007, Available from. <http://www.ommbid.com>.

[2] K. Suzuki, G.C. Chen, Morphological, histological and biochemical studies on a case of systemic late infantile lipidosis (generalized gangliosidosis), J. Neuropathol. Exp. Neurol. 27 (1968) 15–38.

[3] J. Matsuda, O. Suzuki, A. Oshima, A. Ogura, Y. Noguchi, Y. Yamamoto, T. Asano, K. Takimoto, K. Sukegawa, Y. Suzuki, M. Naiki, β-Galactosidase-deficient mouse as an animal model for G_{M1}-gangliosidosis, Glycoconj. J. 14 (1997) 729–736.

[4] C.N. Hahn, M. Martin, M. Schröder, M.T. Vanier, Y. Hara, K. Suzuki, K. Suzuki, A. d'Azzo, Generalized CNS disease and massive G_{M1}-ganglioside accumulation in mice defective in lysosomal acid β-galactosidase, Hum. Mol. Genet. 6 (1997) 205–211.

[5] J.E. Goldman, D. Katz, I. Rapin, D.P. Purpura, K. Suzuki, Chronic GM1 gangliosidosis presenting as dystonia: I. Clinical and pathological features, Ann. Neurol. 9 (1981) 465–475.

[6] J. Matsuda, O. Suzuki, A. Oshima, Y. Yamamoto, A. Noguchi, K. Takimoto, M. Itoh, Y. Matsuzaki, Y. Yasuda, S. Ogawa, Y. Sakata, E. Nanba, K. Higaki, Y. Ogawa, L. Tomonaga, K. Ohno, H. Iwasaki, H. Watanabe, R.O. Brady, Y. Suzuki, Chemical chaperone therapy for brain pathology in G_{M1}-gangliosidosis, Proc. Natl. Acad. Sci. USA 100 (2003) 15912–15917.

[7] Y. Suzuki, S. Ichinomiya, M. Kurosawa, M. Ohkubo, H. Watanabe, H. Iwasaki, J. Matsuda, Y. Noguchi, K. Takimoto, M. Itoh, M. Tabe, M. Iida, T. Kubo, S. Ogawa, E. Nanba, K. Higaki, K. Ohno, R.O. Brady, Chemical chaperone therapy: clinical effect in murine G_{M1}-gangliosidosis, Ann. Neurol. 62 (2007) 671–675.

[8] M. Jeyakumar, R.A. Dwek, T.D. Butters, F.M. Platt, Storage solutions: treating lysosomal disorders of the brain, Nat. Rev. Neurosci. 6 (2005) 1–12.

[9] M.C. Maiuri, E. Zalckvar, A. Kimchi, G. Kroemer, Self-eating and self-killing: crosstalk between autophagy and apoptosis, Nat. Rev. Mol. Cell Biol. 8 (2007) 741–752.

[10] B. Levine, J. Yuan, Autophagy in cell death: an innocent convict? J. Clin. Invest. 115 (2005) 2679–2688.

[11] M. Martinez-Vicente, A.M. Cuervo, Autophagy and neurodegeneration: when the cleaning crew goes on strike, Lancet Neurol. 6 (2007) 352–361.

[12] E. Corcelle, M. Nebout, S. Bekri, N. Gauthier, P. Hofman, P. Poujeol, P. Fenichel, B. Mograbi, Disruption of autophagy at the maturation step by the carcinogen lindane is associated with the sustained mitogen-activated protein kinase/extracellular signal-regulated kinase activity, Cancer Res. 66 (2007) 6861–6870.

[13] R.C. Paraguison, K. Higaki, K. Yamamoto, H. Matsumoto, T. Sasaki, N. Kato, E. Nanba, Enhanced autophagic cell death in expanded polyhistidine variants of HOXA1 reduces PBX1-coupled transcriptional activity and inhibits neuronal differentiation, J. Neuroci. Res. 85 (2007) 479–487.

[14] M. Komatsu, S. Waguri, T. Chiba, S. Murata, J. Iwata, I. Tanida, T. Ueno, M. Koike, Y. Uchiyama, E. Kominami, K. Tanaka, Loss of autophagy in the central nervous system causes neurodegeneration in mice, Nature 441 (2007) 880–884.

[15] T. Hara, K. Nakamura, M. Matsui, A. Yamamoto, Y. Nakahara, R. Suzuki-Migishima, M. Yokoyama, K. Mishima, I. Saito, H. Okano, N. Mizushima, Suppression of basal autophagy in neural cells causes neurogenerative disease mice, Nature 441 (2007) 885–889.

[16] Y. Tanaka, G. Guhde, A. Suter, E.L. Eskelinen, D. Hartmann, R. Lullmann-Rauch, P.M. Janssen, J. Blanz, K. von Figura, P. Saftig, Accumulation of autophagic vacuoles and cardiomyopathy in LAMP-2-deficient mice, Nature 406 (2000) 902–906.

[17] M. Koike, M. Shibata, S. Waguri, K. Yoshimura, I. Tanida, E. Kominami, T. Gotow, C. Peters, K. von Figura, N. Mizushima, P. Saftig, Y. Uchiyama, Participation of autophagy in storage of lysosomes in neurons from mouse models of neuronal ceroid-lipofuscinoses (Batten disease), Am. J. Pathol. 167 (2005) 1713–1728.

[18] T. Fukuda, L. Ewan, M. Bauer, R.J. Mattaliano, K. Zaal, E. Ralston, P.H. Plotz, N. Raben, Dysfunction of endocytic and autophagic pathways in a lysosomal storage disease, Ann. Neurol. 59 (2006) 700–708.

[19] J.J. Jennings Jr, J.H. Zhu, Y. Rbaibi, X. Luo, C.T. Chu, K. Kiselyov, Mitochondrial aberrations in mucolipidosis type IV, J. Biol. Chem. 281 (2006) 39041–39050.
[20] C. Settembre, A. Fraldi, L. Jahreiss, C. Spampanato, C. Venturi, D. Medina, R. Pablo, C. Tacchetti, D.C. Rubinsztein, A. Ballabio, A block of autophagy in lysosomal storage disorders, Hum. Mol. Genet. 17 (2008) 119–129.
[21] C.D. Pacheco, R. Kunkel, A.P. Lieberman, Autophagy in Niemann-Pick C disease is dependent upon beclin-1 and responsive to lipid trafficking defects, Hum. Mol. Genet. 16 (2007) 1495–1503.
[22] J.H. Zhu, F. Guo, J. Shelburne, S. Watkins, C.T. Chu, Localization of phosphorylated ERK/MAP kinases to mitochondria and autophagosomes in Lewy body diseases, Brain Pathol. 13 (2003) 473–481.
[23] P.I. Moreira, S.L. Siedlak, X. Wang, M.S. Santos, C.R. Oliveira, M. Tabaton, A. Nunomura, L.I. Szweda, G. Aliev, M.A. Smith, X. Zhu, G. Perry, Autophagocytosis of mitochondria is prominent in Alzheimer disease, J. Neuropathol. Exp. Neurol. 66 (2007) 525–532.
[24] J.H. Zhu, C. Horbinski, F. Guo, S. Watkins, Y. Uchiyama, C.T. Chu, Regulation of autophagy by extracellular signal-regulated protein kinases during 1-methyl-4-phenylpyridinium-induced cell death, Am. J. Pathol. 170 (2007) 75–86.
[25] A. Yamamoto, L.M. Cremona, J.E. Rothman, Autophagy-mediated clearance of huntingtin aggregates triggered by the insulin-signaling pathway, J. Cell Biol. 172 (2006) 719–731.

MUTATION IN BRIEF

Novel Mutations of the GLA Gene in Japanese Patients with Fabry Disease and Their Functional Characterization by Active Site Specific Chaperone

Masaaki Shimotori[1], Hiroki Maruyama[2*], Gen Nakamura[1], Takayuki Suyama[3], Fumiko Sakamoto[3], Masaaki Itoh[3], Shigeaki Miyabayashi[4], Takahiro Ohnishi[5], Norio Sakai[6], Mari Wataya-Kaneda[7], Mitsuru Kubota[8], Toshiyuki Takahashi[9], Tatsuhiko Mori[10], Katsuhiko Tamura[11], Shinji Kageyama[12], Nobuo Shio[12], Teruhiko Maeba[13], Hirokazu Yahagi[14], Motoko Tanaka[15], Masayo Oka[16], Hitoshi Sugiyama[17], Toshiyuki Sugawara[18], Noriko Mori[19], Hiroko Tsukamoto[20], Keiichi Tamagaki[21], Shuuji Tanda[22], Yuka Suzuki[23], Chiya Shinonaga[23], Jun-ichi Miyazaki[24], Satoshi Ishii[25], and Fumitake Gejyo[1]

[1]Division of Clinical Nephrology and Rheumatology, Niigata University Graduate School of Medical and Dental Sciences, Niigata, Japan; [2]Department of Clinical Nephroscience, Niigata University Graduate School of Medical and Dental Sciences, Niigata, Japan; [3]Department of Dermatology, Niigata University School of Medicine, Niigata, Japan; [4]Sendai Medical Center, Sendai, Japan; [5]Yamada Red Cross Hospital, Tokai, Japan; [6]Division of Internal Medicine, Osaka University Graduate School of Medicine Department of Pediatrics, Suita, Japan; [7]Department of Dermatology Course of Molecular Medicine, Osaka University, Graduate School of Medicine, Suita, Japan; [8]Department of Pediatrics, Hokkaido University School of Medicine, Sapporo, Japan; [9]Department of Cardiology, Pulmonology, and Nephrology Course of Internal Medicine and Therapeutics Yamagata University School of Medicine, Yamagata, Japan; [10]Third Department of Medicine, Osaka Medical College, Osaka, Japan; [11]Shinonoi General Hospital, Shinonoi, Japan; [12]Sio Urological Clinic, Aoi, Japan; [13]Asao Kidney Clinic, Kawasaki, Japan; [14]Osaki Citizen Hospital, Cardiovascular Medicine, Osaki, Japan; [15]Department of Nephrology, Akebono Clinic 5-1-1, Shirafuji, Kumamoto, Japan; [16]Department of Medicine and Clinical Science, Graduate School of Medical Sciences, Kyushu University, Fukuoka, Japan; [17]Department of Medicine and Clinical Science Okayama University Graduate School of Medicine, Dentistry, and Pharmaceutical Sciences, Okayama, Japan; [18]Mutsu General Hospital Department of Cardiology, Mutsu, Japan; [19]Kidney Center, Shizuoka General Hospital, Shizuoka, Japan; [20]Depatment of Pediatrics, Sumitomo Hospital, Osaka, Japan; [21]Department of Nephrology, St. Luke's International Hospital, Tokyo, Japan; [22]Omihachiman Community Medical Center, Shiga, Japan; [23]Department of Pediatrics, School of Medicine Ehime University, Ehime, Japan; [24]Division of Stem Cell Regulation Research, Osaka University Medical School G6, Suita, Japan; [25]Department of Agricultural and Life Sciences, Obihiro University of Agriculture and Veterinary Medicine, Obihiro, Japan

*Correspondence to: Hiroki Maruyama, MD, PhD, FJSIM. Department of Clinical Nephroscience Niigata University Graduate School of Medical and Dental Sciences, 1-757 Asahimachi-dori, Niigata 951-8120, Japan; Tel.: +81-25-227-0436; Fax; +81-25-227-0437; E-mail: hirokim@med.niigata-u.ac.jp

Communicated by William S. Sly

Fabry disease is an X-linked recessive inborn metabolic disorder caused by a deficiency of the lysosomal enzyme α-galactosidase A (EC 3.2.1.22). The causative mutations are diverse, include both large rearrangements and single-base substitutions, and are dispersed

Received 22 May 2007; accepted revised manuscript 26 September 2007.

DOI: 10.1002/humu.9520

throughout the 7 exons of the α-galactosidase A gene (*GLA*). Mutation hotspots for Fabry disease do not exist. We examined 62 Fabry patients in Japan and found 24 *GLA* mutations, including 11 novel ones. A potential treatment reported for Fabry disease is active site specific chaperone (ASSC) therapy using 1-deoxygalactonojirimycin (DGJ), an inhibitor of α-galactosidase A, at subinhibitory concentrations. We transfected COS-7 cells with the 24 mutant *GLA*s and analyzed the α-galactosidase A activities. We then treated the transfected COS-7 cells with DGJ and analyzed its effect on the mutant enzyme activities. The activity of 11 missense mutants increased significantly with DGJ. Although ASSC therapy is useful only for misfolding mutants and therefore not applicable to all cases, it may be useful for treating many Japanese patients with Fabry disease.

KEY WORDS: α-galactosidase A; GLA; lysosomal storage disease; 1-deoxygalactonojirimycin; chaperone therapy

INTRODUCTION

Fabry disease (FD; MIM# 301500) is a pan-ethnic, X-linked, lysosomal storage disorder caused by a deficiency in the lysosomal enzyme α-galactosidase A (EC 3.2.1.22) (Brady et al., 1967). Human α-galactosidase A is a homodimeric glycoprotein with three N-linked oligosaccharide chains on each subunit. Enzyme deficiency results in a systemic lysosomal accumulation of glycolipids, primarily globotriosylceramide (Gb3), in the vascular endothelium and other tissues. In the classical form of the disease, the patient develops angiokeratoma, hypohidrosis, and episodic pain crises in the extremities during childhood or adolescence. With advancing age, the morbidity of renal failure, cardiac disease, and early onset of stroke increases. The severity of the clinical manifestations depends on the amount of residual α-galactosidase A activity. Hemizygous male patients with no or very low α-galactosidase A activity usually have severe clinical symptoms and die as young adults. Heterozygous female Fabry patients exhibit a wide range of severity, from a virtually symptom-free course (Marguery et al., 1993) to one comparable to that of their male counterparts (Whybra et al., 2001), although they usually have no symptoms or very mild manifestations.

We examined Fabry patients in Japan and sequenced the patients' *α-galactosidase A* gene (*GLA*) (MIM# 300644). To analyze the mutant α-galactosidase A activities, we transfected COS-7 cells with the mutant *GLA*s. In addition, since 1-deoxygalactonojirimycin (DGJ) stabilizes the α-galactosidase A conformation and improves its stability (Asano et al., 2000; Ishii et al., 2000; Yam et al., 2006), we added DGJ to the incubation medium and examined its effect on the mutant α-galactosidase A activities.

MATERIALS AND METHODS

Patients

We examined 62 Fabry patients from 31 unrelated families. Diagnosis was based on reduced or absent α-galactosidase A activity and typical signs and symptoms of the disease. We received approval to use the patients' DNA for this study from The Ethics Committee on Genetics of the Niigata University School of Medicine, and obtained informed consent from the patients.

Mutation analysis

Blood samples obtained from patients with Fabry disease were transferred into blood-collecting tubes containing ethylene diamine tetraacetic acid (EDTA) and stored at 4°C. Unlike heparin, EDTA does not inhibit the activity of reverse transcriptase, which is used for the reverse transcriptase polymerase chain reaction (RT-PCR). The human *GLA* consists of 7 exons. We found it difficult to obtain full-length *GLA* cDNA (RefSeq BC_002689.2) by performing a single RT-PCR. We therefore obtained exon 1 and exon 7 by PCR from genomic DNA, and the region between exons 1 and 7, containing the full-length exons 2-6 by RT-PCR, from total RNA.

White blood cells were collected using Lymphoprep (Axis-Shield PoC, Oslo, Norway). The genomic DNA of the white blood cells was isolated using an automatic isolation system (NA1000; Kurabo, Osaka, Japan) within 1 week after blood sampling and stored at -20°C until use.

To determine the sequence of exons 1 and 7 of *GLA*, we performed PCR on genomic DNA with the following specific primers: Sense Ex1-1(+), 5'-CCAGTTGCCAGAGAAACA-3'; Antisense Ex1-2(-), 5'-GAGACTCTCCAGTTCCC-3'; Sense Ex7-5(+), 5'-ACAAGTGCTTGATAGTTCTGA-3'; Antisense Ex7-6(-), 5'-CAGGAAGTAGTAGTTGGCAA-3'. The PCR protocol consisted of 2 min at 94°C, then 30 cycles of 15 sec at 94°C, 30 sec at 59°C, and 30 sec at 68°C with KOD-Plus DNA polymerase (Toyobo, Osaka, Japan). The lengths of the expected products were 390 bp for exon 1 and 420 bp for exon 7. The PCR products were analyzed by 2% NuSieve GTG agarose (Takara, Shiga, Japan) gel electrophoresis and then eluted using the Gene Clean Spin Kit (Q-BIOgene, Irvine, CA, U.S.A.).

To determine the sequence of the cDNA region of *GLA* that included exons 2 to 6, we first amplified it by RT-PCR. We generated first-strand cDNA by RT (ReverTra Ace -α-, Toyobo) using random 9-mers. The reaction consisted of 10 min at 30°C, 20 min at 42°C, 5 min at 99°C, and 5 min at 4°C. To amplify the cDNA of *GLA*, we performed the first PCR with specific primers as follows: 5' #1 primer: 5'-TATGCTGTCCGGTCACC-3', #66 (AG66) primer: 5'-TTAAAGTAAGTCTTTTAATGACAT-3'. The PCR protocol consisted of 2 min at 94°C, then 30 cycles of 15 sec at 94°C, 30 sec at 55°C, and 1 min 30 sec at 68°C with KOD-Plus DNA polymerase (Toyobo). The first PCR products were purified using the QIAquick PCR Purification Kit (Qiagen GmbH, Hilden, Germany). The length of the expected products was 1.3 kbp. To amplify the *GLA* cDNA, we performed a second (nested) PCR with the following specific primers: cDNA#1, 5'-TTGGCAAGGACGCCTAC-3'; cDNA#2, 5'-TGCGATGGTATAAGAGCG-3'. The PCR protocol consisted of 2 min at 94°C, then 30 cycles of 15 sec at 94°C, 30 sec at 55°C, and 1 min at 68°C with KOD-Plus DNA polymerase (Toyobo). The length of the expected product was 1 kbp. The PCR products were analyzed by 2% NuSieve GTG agarose (Takara) gel electrophoresis and then eluted using the Gene Clean Spin Kit (Q-BIO gene).

We analyzed both strands of the *GLA* sequence in the PCR and RT-PCR products by direct sequencing using an ABI PRISM 3100 Genetic Analyzer (Applied Biosystems, Foster, CA, U.S.A.).

Construction of pKSCX-*GLA*

We constructed plasmid pKSCX-*GLA* by inserting the normal human *GLA* cDNA in pCXN2Gal (Ishii et al., 1993) into the unique EcoRI site of the pKSCX expression vector, which bears the cytomegalovirus immediate-early enhancer/chicken β-actin hybrid promoter, and the kanamycin-resistance gene for selection (Niwa et al., 1991). We confirmed the pKSCX-GLA construct by sequencing both DNA strands.

Construction of pKSCX-mutant-*GLA*

To create point mutations or to delete or insert single or multiple amino acids, we used the QuickChange site-directed mutagenesis kit (Stratagene, La Jolla, CA, U.S.A.) (Yasuda et al., 2004). Because pKSCX contains many GC-rich sequences, we constructed plasmid pCI-*GLA* by inserting the normal human *GLA* cDNA of pCXN2Gal (Ishii et al., 1993) into the unique *Eco*RI site of the pCI mammalian expression vector (Promega, Madison, WI, U.S.A.). We then used pCI-*GLA* as the mutagenesis template. We designed specific primer pairs according to each mutation. To clone the mutant-*GLA* cDNA derived from patients with Fabry disease, we incorporated the mutation into the pCI-*GLA* cDNA using the site-directed mutagenesis kit with the specific primer pairs. We confirmed the mutant *GLA*s by sequencing both DNA strands. We digested the pCI-mutant-*GLA* with *Eco*RI, eluted the *Eco*RI-*Eco*RI fragment containing the mutant-*GLA* cDNA, and ligated it into the like-digested cloning site of pKSCX, yielding pKSCX-mutant-*GLA*.

Cell culture and transfection

We prepared pKSCX-*GLA* or pKSCX-mutant-*GLA* using the Qiagen EndoFree plasmid Giga kit (Qiagen GmbH) (Maruyama et al., 2000), as described previously, and then subjected it to ethanol precipitation.

COS-7 cells (Originator, Gluzman Y; Riken Cell Bank, RCB 0539) were grown at 37°C in Dulbecco's modified Eagle's medium (DMEM; Gibco, Rockville, MD, U.S.A.) containing 10% fetal bovine serum (FBS; Gibco) (Yasuda et al., 2003). The cells were harvested by trypsin treatment, washed in 10 ml of DMEM containing 10% FBS, and resuspended at 5×10^6 cells/ml in DMEM containing 10% FBS. The cells were

transfected by the LipofectAMINE 2000 method (Invitrogen, Carlsbad, CA, U.S.A.), according to the manufacturer's instructions. The cells were cultured in DMEM containing 10% FBS at 37°C and 5% CO_2. The COS-7 cells were transfected with pKSCX plasmid *in vitro* using the LipofectAMINE2000 cationic lipid reagent. Briefly, 8 μg of DNA (4 μg pKSCX-mutant-*GLA* and 4 μg pKSCX-luciferase) were mixed with 20 μL of LipofectAMINE2000 reagent and added to the medium in 60-mm dishes. After the transfection, the transformants were cultured in 5 ml of DMEM containing 10% FBS with or without 10 μM DGJ (Sigma Chemical, St. Louis, MO, U.S.A.) at 37°C for 3 days before the enzyme assay. The cells were harvested by trypsin treatment, rinsed with phosphate-buffered saline, and homogenized with 0.2 ml of water with a Physcotron (NS-310E, Niti-on, Chiba, Japan). The sample was then subjected to centrifugation at 10000×g for 5 min. The water-soluble extract was used as the enzyme source.

α-Galactosidase A activity assay

The α-Galactosidase A activity of the water-soluble extract was determined using an artificial substrate, 4-methyl-umbelliferyl α-D-galactopyranoside (Nacalai Tesque, Kyoto, Japan), as described previously (Fan et al., 1999). The protein content of the water-soluble extract was measured by the method of Lowry (DC protein assay; Bio-Rad, Hercules, CA, U.S.A.).

Luciferase assay

Briefly, 20 μl of the water-soluble extract was added to 100 μl of firefly luciferin solution (PicaGene, Toyo Ink, Tokyo, Japan). The luciferase activity was measured for 10 sec using a luminometer (GENE LIGHT, Microtec Nition, Chiba, Japan), according to the manufacturer's instructions.

Statistical analysis

The data are presented as the mean values ± the standard deviation of the mean. We analyzed all data using the Statcel2 Microsoft Office Excel Add-in Software (Hisae Yanai, Department of Mathematics, Faculty of Science Saitama University). Statistical significance was evaluated using the unpaired *t*-test. We considered *P* values of < 0.05 to be statistically significant.

RESULTS AND DISCUSSION

We detected 24 mutations in 62 Fabry patients from 31 unrelated families in Japan (Table 1). The patients' clinical characteristics are shown in Table 2; the numbers correspond to those of the mutant *GLA*s in Table 1. The mutations consisted of 17 missense substitutions (p.M42V, p.E66Q, p.M76T, p.D93V, p.R112H, p.S148N, p.P205T, p.D231V, p.S235F, p.G258V, p.G260A, p.T282A, p.K308N, p.Q312R, p.G328R, p.L403S, p.T410P), 3 nonsense substitutions (p.S102X, p.R227X, p.W399X), 2 small deletions (c.718_719delAA, c.1020delG), 1 insertion (c.323_324insCAGA), and 1 double missense mutation (p.E66Q, p.R112C). Importantly, 11 of the mutations (p.M76T, p.D231V, p.S235F, p.G258V, p.T282A, p.K308N, p.Q312R, p.L403S, p.T410P, p.S102X, c.323_324insCAGA) were novel. The mutant *GLA* p. E66Q, which is a G-to-C transversion at nucleotide 196 (cDNA) of exon 2, was observed in seven putatively unrelated families, and the mutant *GLA* c.1020Gdel-deletion, was observed in two putatively unrelated families.

To date, more than 20 mutant *GLA*s have been reported in Japan (Takata et al., 1997; Okumiya et al., 1995; Miyamura et al., 1996). Of the 24 mutant *GLA*s we examined, 4 (p. E66Q, p. G260A, p. G328R, c. 718_719delAA) are the same as the known mutant *GLA*s in Japan, and 20 are different. Therefore, in the present study, we examined over half the mutant *GLA*s in Japan.

To examine the activities of the α-galactosidase A produced by these mutant genes, COS-7 cells were transfected with the mutant *GLA*s and cultured with or without 10 μM DGJ for 3 days. All the mutant-α-galactosidase A activities were low, with 0.1% to 50% of the mean normal activity. We examined the relationship between the enzyme activity and clinical symptoms. As expected from previous studies, a one-seventh value of normal α-galactosidase A activity was sufficient to suppress clinical symptoms, and 8 of the 24 mutations reached an activity at least one-seventh that of normal α-galactosidase A activity with DGJ treatment (Table 2) (Nakao et al., 1995; Nakao et al., 2003; Yoshitama et al., 2001). The patients with a one-seventh value of normal α-galactosidase A activity or more did not exhibit the classic symptoms of the disease (angiokeratoma, hypohidrosis,

and episodic pain crises), nor did they develop renal failure and/or cardiac disease later in life (Nakao et al., 1995; Nakao et al., 2003; Yoshitama et al., 2001).

Some mutant-α-galactosidase A variants form aggregates in the endoplasmic reticulum (ER), due to their failure to fold properly during synthesis, and they may lose their enzyme activity. Such mutant-α-galactosidase A variants may be degraded by the ER quality control system (Yam et al., 2006). Moreover, misfolded α-galactosidase A variants appear to stay within the ER regardless of their catalytic competence, leading to their possible degradation or aggregate formation. As a result, mutant α-galactosidase A variants with defective folding tend to be retained in the ER and not reach the lysosomes, where the enzyme functions. DGJ functions as an active-site-specific chaperone (ASSC) to stabilize the conformation of mutant-α-galactosidase A variants and preserve at least some of their enzyme activity. In some cases, DGJ allows mutant-α-galactosidase A variants to pass through the ER quality control system and be sorted into lysosomes, resulting in an increase in the mutant's α-galactosidase A activity. This suggests that the stability of mutant α-galactosidase A is a critical factor that determines its further transportation and function as residual enzyme activity. However, DGJ does not have a measurable effect on all mutant α-galactosidase A activities, particularly those with frame-shift or early termination mutations.

In this study, the activities of 11 of the 24 α-galactosidase A mutants significantly increased after incubation with 10 μM DGJ for 3 days (Table 1). The activity of 11 missense mutants significantly increased with DGJ treatment, while that of the other missense, and the nonsense, insertion, and deletion mutants did not increase. Because the No. 7 mutation causes the incorrect synthesis of most of the protein, including the active site, the apparent enzyme activity of No. 7, 4% of the normal enzyme activity, may be experimental noise. Therefore, some of the other mutations with less than 4% enzyme activity need to be interpreted carefully. Nevertheless, these findings indicate that although ASSC therapy is not applicable to all patients with Fabry disease, many Japanese patients might respond to such treatment. Importantly, a preliminary study of DGJ use in transgenic mice showed no general signs of toxicity (Fan et al., 1999), supporting this compound's promise as a treatment for human Fabry disease.

Our findings support the potential usage of ASSC as an alternative treatment for Fabry disease. It is likely that by correcting the trafficking defect with DGJ, the misfolded α-galactosidase A variants are directed to lysosomes, thereby increasing their residual enzymatic activities. Our results showed that DGJ specifically affects misfolded α-galactosidase A, since it reproducibly increased the activity of different *GLA* variants. We also showed that DGJ causes normal α-galactosidase A activity to increase, although the reason is not known. Therefore, DGJ may be a useful treatment for every heterozygous patient.

Recently, enzyme replacement therapy (ERT) was approved for patients with Fabry disease: two recombinant glycoprotein products, Replagal® (Transkaryotic Therapies, Cambridge, MA, U.S.A.) and Fabrazyme® (Genzyme, Cambridge, MA, U.S.A.), are now available (Goi et al., 2005; Hoffmann et al., 2006). Because kidney and heart involvements are important causes of the morbidity and mortality in patients with Fabry disease, they should be the main targeted organs in therapies designed to treat it. However, many investigations have reported that in Fabry disease the kidney and heart are highly resistant to ERT with either enzyme treatment (Brady et al., 2001; Ioannou et al., 2001). Furthermore, most of the injected enzyme is delivered to the liver and has difficulty reaching other organs, such as the kidney and heart (Lee et al., 2003; Sakuraba et al., 2006). In addition, the Gb3 in the Fabry mouse kidney is highly resistant to ERT by systemic intravenous injection. In ERT of the Fabry mouse, most (65~70%) of the injected enzyme is recovered in the liver, and less than roughly 1% of the injected dose is detected in the kidney and heart (Lee et al., 2003). An examination of ERT in the Fabry mouse also showed that only a very small quantity of the recombinant enzyme remains in tissues hours after the infusion.

DGJ treatment, in contrast, increased the enzyme activity of normal α-galactosidase A and of several mutant-α-galactosidase A variants (Table1, No.1, 4, 8, 10, 13, 15, 16, 17,18, 19, 23) enough to extend the persistence of enzyme activity *in vitro*. Using DGJ as an ASSC may resolve the problems caused by mutant α-galactosidase A effectively. Increasing the activity of both normal and mutant α-galactosidase A with DGJ treatment may prove clinically useful.